JOURNAL OF MATERIALS SCIENCE 31 (1996) 741–747

Property–microstructure correlation in *in situ* formed Al_2O_3, TiB_2 and Al_3Ti mixture-reinforced aluminium composites

Z. Y. MA, J. H. LI, S. X. LI, X. G. NING, Y. X. LU, J. BI
Laboratory of Atomic Imaging of Solids, Institute of Metal Research, Chinese Academy of Sciences, Shenyang 110015, Republic of China

The *in situ* formed Al_2O_3, TiB_2 and Al_3Ti mixture-reinforced aluminium composites were successfully fabricated by the reaction sintering of the TiO_2–B–Al system in a vacuum. With increasing boron content in the TiO_2–B–Al system, the amount of generated TiB_2 in the composites increased and Al_3Ti content decreased. At the same time the distribution uniformity of the *in situ* formed Al_2O_3 and TiB_2 particulates was obviously improved, and the size of the Al_3Ti particles was reduced. The *in situ* Al_2O_3 and TiB_2 particulates had sizes from 0.096–1.88 μm. The interface between the *in situ* formed particulates and the aluminium matrix was clean, and no consistent crystallographic orientation relationship was found. The strength and elastic modulus of the composites was significantly improved by lowering the Al_3Ti content. When the boron content in the TiO_2–B–Al system rose, the morphology of the tensile fracture surface of the composites was changed from large fractured Al_3Ti blocks and fine dimples, to fine dimples and pulled-out particulates. The strengthening and fracture of the composites have been modelled.

1. Introduction

Aluminium alloys discontinuously reinforced with ceramic particulates, whiskers or short fibres are currently being developed for various high-performance applications. To improve the interfacial compatibility and avoid serious interfacial reaction, various new processing techniques are being used to fabricate the high-performance composites. A process termed the XD™ technique [1] has been developed to fabricate *in situ* ultrafine ceramic particle-reinforced metal matrix composites. The basic principle of this technique is that the ultrafine ceramic particles are formed *in situ* by the exothermal reaction between elements or between element and compound. Using this approach, the metal matrix composites composed of a wide variety of matrix materials (including aluminium, iron, copper, lead, nickel and titanium) and second-phase particles (including borides, carbides, nitrides and their mixtures) have now been produced [1]. The *in situ* composites exhibit improved strength at elevated temperature as well as enhanced wear and fatigue resistance [1, 2].

Recently, Al_2O_3 particle-reinforced aluminium composite formed *in situ* through the reaction between TiO_2 and aluminium has been investigated [3, 4]. According to the reaction formula between TiO_2 and aluminium, if 1 volume of Al_2O_3 is formed, about 2.26 volumes of Al_3Ti will be generated. The properties of the *in situ* formed Al_2O_3 particle-reinforced aluminium composite are difficult to tailor or control due to the inevitable existence of a large amount of brittle Al_3Ti intermetallic compound. In a previous paper [5], the *in situ* formation of $Al_2O_3 \cdot Al_3Ti$/Al and $Al_2O_3 \cdot TiB_2$/Al composites were investigated. It was indicated that the properties of the composites can be improved by eliminating Al_3Ti through the incorporation of boron. In present work, different contents of boron were incorporated into the TiO_2–Al system, and the relationship between the properties and microstructure of the composites was studied.

2. Experimental procedure

Atomized aluminium powder (99.6% purity), TiO_2 powder (98.0% purity) and boron powder (99.0% purity) with an average size of 40, 3, 2 μm, respectively, were used as raw materials. The composites were fabricated by a powder metallurgy technique, whereby aluminium, TiO_2 and boron powders were ball-milled for 8 h. During powder blending, TiO_2 powder of the same weight was added in samples 8, 4, 5 and 3 in order to form 10.5 vol % Al_2O_3 in the above composites, and different contents of boron powder were added to these four samples to give a B/TiO_2 molecular ratio of 0, 4/3, 5/3 and 2/1 in samples 8, 4, 5 and 3, respectively, so that the composites containing different contents of TiB_2 and Al_3Ti could be produced. The cold-compacted powder mixture was heated to above 800 °C in a vacuum and maintain for 10 min, then cooled down to 600 °C and hot-pressed. The pressed billets were extruded at an extrusion ratio of 20:1 at 420 °C. The metallographic observations and

0022–2461

X-ray diffraction analyses on the mechanically polished specimens were carried out. Sample 3 was solved in dilute hydrochloric acid; the solution with ceramic particulates was diluted and filtrated. The filtrated particulates were dried, then examined on a quantitative metallograph. The thin foils for transmission electron microscope (TEM) were prepared by the ion-milling technique. The foils were examined on a JEM 2000EX II high-resolution TEM (HRTEM). Tensile specimens, with a gauge diameter of 4 mm and a gauge length of 10 mm, were machined from the extruded rods, and tested at a strain rate of $8.3 \times 10^{-4}\ s^{-1}$. The tensile fracture surfaces were observed on a scanning electron microscope (SEM). The elastic modulus of the composites was measured by a resonance method.

3. Results and discussion

In the TiO_2–B–Al system, the chemical reactions take place as follows

$$3TiO_2 + 4Al \rightarrow 2Al_2O_3 + 3[Ti] \quad (1)$$

$$[Ti] + 3Al \rightarrow Al_3Ti \quad (2)$$

$$[Ti] + 2B \rightarrow TiB_2 \quad (3)$$

All the reactions are exothermic. Therefore, when the temperature of the system reaches the starting temperature of the reaction between TiO_2 and aluminium, the heat released by the reaction rapidly raises the temperature of the system, and promotes the reactions between titanium and boron or aluminium. All reactions will be finished in a short time. According to the previous investigations on the Ti–B–Al system [2, 6], the reaction between titanium and boron occurs much more easily than that between titanium and aluminium. Therefore, there would be different contents of TiB_2 and Al_3Ti in the composites with increasing boron content in the TiO_2–B–Al system. If the boron in TiO_2–B–Al system reacts completely with the titanium displaced from the reaction between TiO_2 and aluminium, different contents of TiB_2 and Al_3Ti in the composites can be generated (Table I). With increasing boron content in the TiO_2–B–Al system, the amount of the TiB_2 generated increases and the Al_3Ti content falls. When the molecular ratio of B/TiO_2 is 2/1, the 9.5 vol %TiB_2 will be formed *in situ* and the generation of Al_3Ti will be completely inhibited, provided that the titanium displaced from the reaction between TiO_2 and aluminium reacts completely with boron.

The X-ray diffractograph (XRD) of the composites is shown in Fig. 1. Aluminium, Al_2O_3 and Al_3Ti peaks are seen in the XRD of sample 8 (Fig. 1a); indicating that the reaction between TiO_2 and aluminium has taken place to form Al_3Ti. According to the reaction formula between TiO_2 and aluminium, the formation of 1 volume of Al_2O_3 will be followed by 2.26 volumes of Al_3Ti, so the intensity of the Al_3Ti peaks in sample 8 is much higher than that of Al_2O_3 peaks. When boron is incorporated into the TiO_2–Al system, TiB_2 peaks appear and the intensity of the Al_3Ti peaks is significantly weakened (Fig. 1b), which is further reduced with increasing content of boron in the TiO_2–B–Al system (Fig. 1c). When the molecular ratio of B/TiO_2 reaches 2/1, the Al_3Ti diffraction lines disappear from the XRD (Fig. 1d), indicating that the Al_3Ti is basically eliminated in sample 3. In the investigation on the Ti–B–Al system, the formation of TiB_2 was accompanied by a certain amount of Al_3Ti [6]. These results indicate that the titanium displaced from fine TiO_2 is much more active in the reaction between titanium and boron in comparison with the coarse titanium particles.

Metallographic observations indicated that the microstructure of the composites was quite different. In sample 8, the irregular white blocks with a size of about 20 μm were Al_3Ti, and their size was much greater than that of the added TiO_2 particles (Fig. 2a). The fine grey particulates with a size of about 1 μm were Al_2O_3. The greyish zone was the aluminium matrix. It can be noted that the distribution of the Al_3Ti blocks and Al_2O_3 particulates in the aluminium matrix was obviously non-uniform; there were also

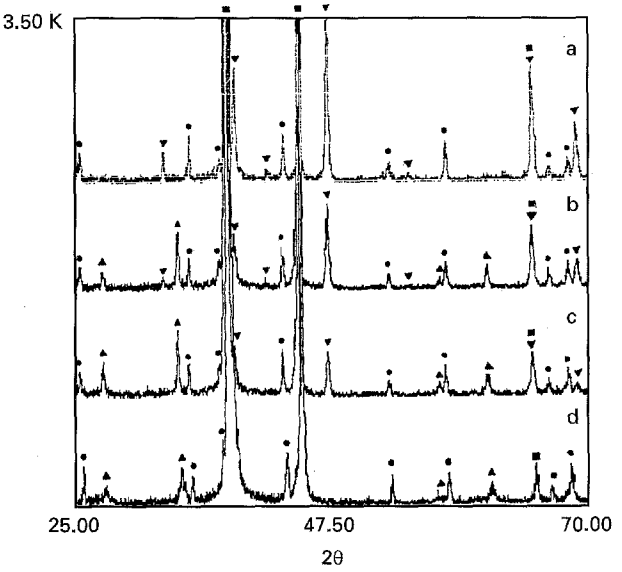

Figure 1 X-ray diffractographs of the composites: (a) sample 8, (b) sample 4, (c) sample 5, (d) sample 3. (●) Al_2O_3, (▼) Al_3Ti, (▲) TiB_2, (■) Al.

TABLE I Content of generated phases (vol %)

Sample	Al_3Ti	Al_2O_3	TiB_2	$Al_2O_3 + TiB_2$	$Al_3Ti + Al_2O_3 + TiB_2$
8	23.73	10.50	0	10.50	34.23
4	7.92	10.50	6.34	16.84	24.76
5	3.95	10.50	7.91	18.41	22.36
3	0	10.50	9.50	20.00	20.00

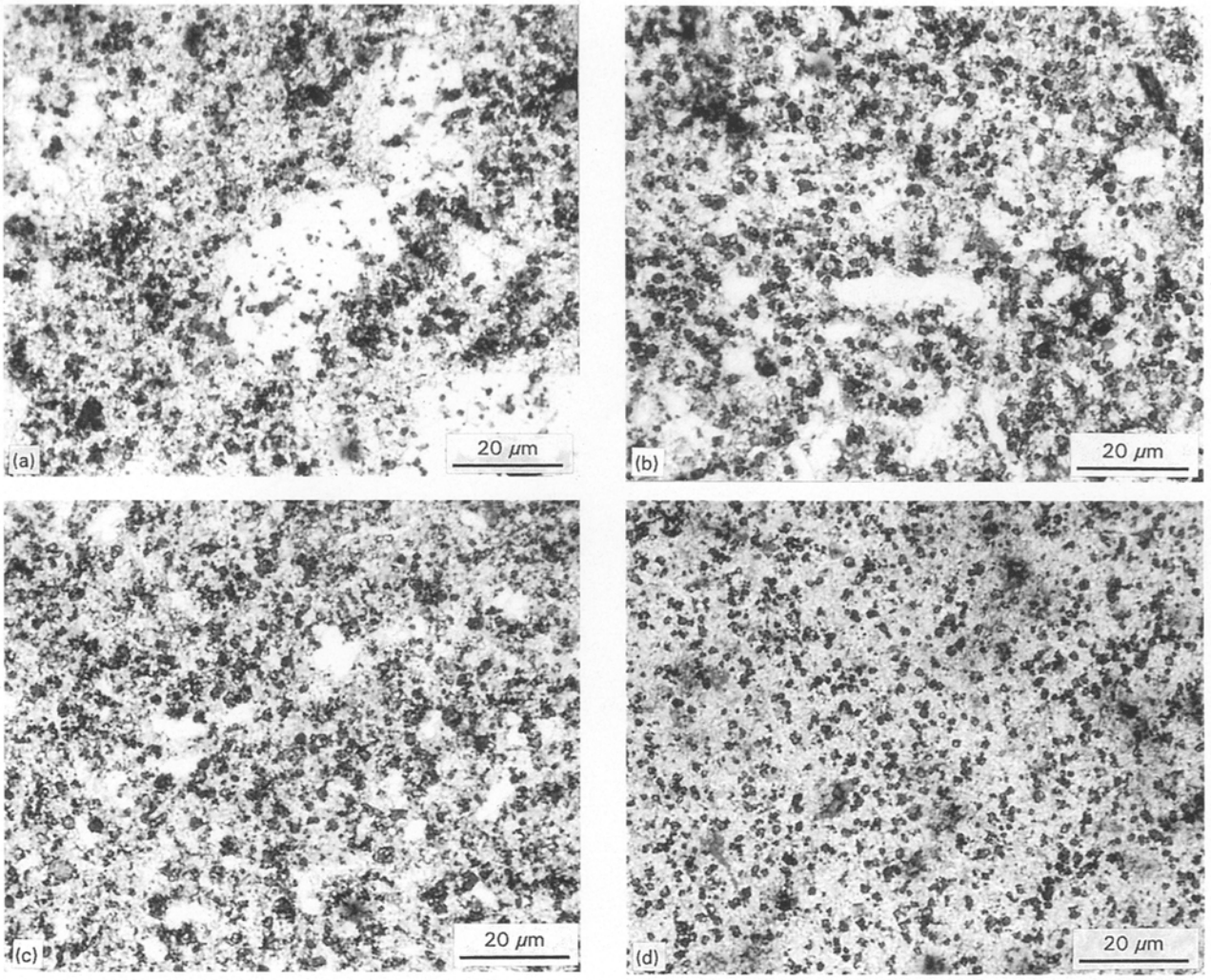

Figure 2 Metallographs of the composites: (a) sample 8, (b) sample 4, (c) sample 5, (d) sample 3.

a few Al_2O_3 particulates in Al_3Ti blocks, and some micropores were also found. After boron was incorporated into the TiO_2–Al system, the amount of Al_3Ti blocks decreased, their size was reduced to about 10 μm, the amount of the fine particulates increased, and the distribution of the Al_3Ti blocks and the fine particulates was improved (Fig. 2b). With increasing boron content to a B/TiO_2 molecular ratio of 5/3 in the TiO_2–B–Al system, the amount of Al_3Ti blocks was further reduced (Fig. 2c). Al_3Ti blocks with a size of about 5 μm and fine particulates were uniformly distributed in the aluminium matrix. When the boron reached a B/TiO_2 molecular ratio of 2/1, the Al_3Ti blocks disappeared and the distribution uniformity of the fine Al_2O_3 and TiB_2 particulates in the aluminium matrix was further improved (Fig. 2d).

Quantitative metallography examinations on the ceramic particulates taken from sample 3 indicated that the Al_2O_3 and TiB_2 particulates had an average size of 0.31 ± 0.04 μm; the largest size of the particulates was 1.88 μm, and the smallest size 0.096 μm. Some much smaller particulates cannot be resolved by quantitative metallography.

TEM observations indicated that a large amount of the *in situ* formed particulates had a size of about 50 nm (Fig. 3), though quantitative metallographic examinations indicated that the particulates had a size

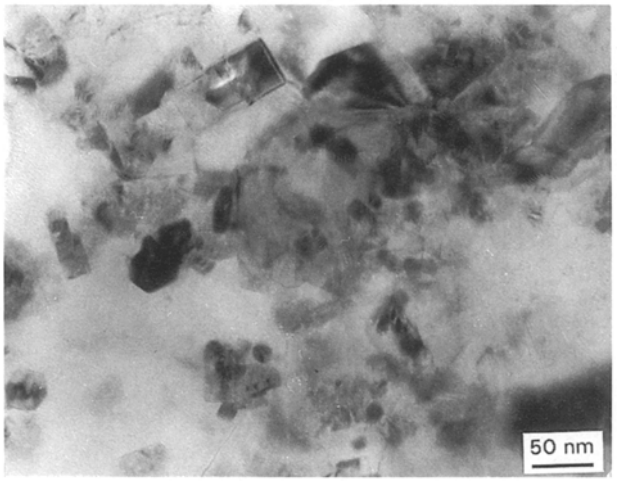

Figure 3 TEM image of sample 3.

from 0.096–1.88 μm. The TiB_2 particulate in Fig. 4 is only 15 nm. These observations indicate that the *in situ* formed particulates are very fine, and their size is much less than that of *in situ* TiC particulates [7, 8] and TiB_2 particulates [2]. The ultrafine particulates could contribute to the increase in composite strength. The interface between the particulates and the aluminium matrix was clean and without a transitional layer between them. No consistent crystallographic

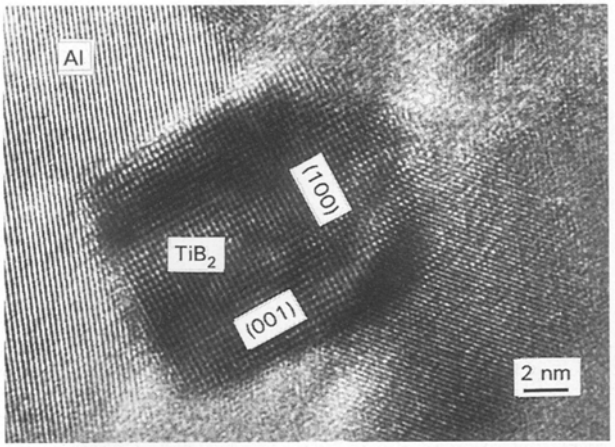

Figure 4 HRTEM image of sample 3.

orientation relationship between particulates and aluminium matrix was found.

Table II shows the properties of the composites. The tensile strength of sample 8 is only 145 MPa, and increases a little over that of the aluminium matrix (about 100 MPa), which demonstrates that the large amount of Al_3Ti blocks existing in sample 8 have no obvious strengthening effect on the aluminium matrix. The ductility of the composite is also lower. When 6.34 vol %TiB_2 is formed and the content of Al_3Ti is reduced to 7.91 vol % due to the addition of boron, the tensile strength of the composite is significantly improved and reaches 311 MPa. With increasing boron content in the TiO_2–B–Al system, the strength of the composite increases further. When the molecular ratio of the B/TiO_2 is 2/1, the tensile strength of the composite (sample 3) reaches 381 MPa and increases by about 163% over that of sample 8 due to the elimination of the brittle Al_3Ti blocks. With increasing the TiB_2 content, the ductility of the composites can be improved by the reduction of the blocky Al_3Ti in the composites, on the other hand, the ductility decreases due to the increase in the strength of the composites. Therefore, the ductility of the composites varies slightly, decreases first and then increases. The ductility of sample 3 with high strength is somewhat superior to that of sample 8, due to complete elimination of the brittle Al_3Ti. The elastic modulus of sample 8 is only 78.9 GPa, a little above that of the aluminium matrix, indicating that a large amount of the blocky Al_3Ti in sample 8 does not increase the elastic modulus of the material. The slight increase in elastic modulus is attributed to 10.5 vol %Al_2O_3 particulates. When the 6.34 vol %TiB_2 is formed and the content of the Al_3Ti is reduced to 7.91 vol %, the elastic modulus of the composite (sample 4) reaches 107.0 GPa, and is significantly improved over that of sample 8.

Fig. 5 shows the temperature dependence of tensile strength for the composites. The strength of sample 8 decreases slowly and linearly with increasing test temperature. After incorporating boron into the TiO_2–Al system, the tensile strength of the composites (samples 4, 5 and 3) is significantly improved at the temperatures ranging from room temperature to 400 °C, but decreases more rapidly than that of sample

TABLE II Properties of the composites

Sample	UTS (MPa)	YS (MPa)	El (%)	*E* (GPa)
8	145	110	5.42	78.9
4	311	271	4.83	107.0
5	328	301	4.70	–
3	381	340	5.53	–

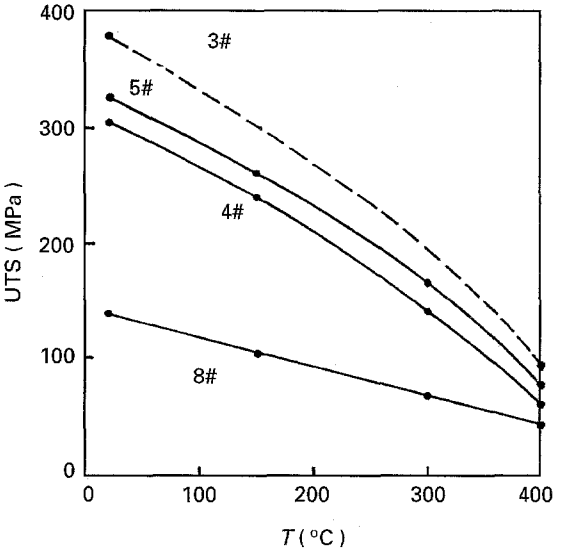

Figure 5 Temperature dependence of tensile strength for the composites.

8 with increasing temperature, which indicates that the Al_3Ti is somewhat beneficial to the elevated temperature strength of the composites, but the effect is small due to the large size of Al_3Ti. The composites (samples 4, 5 and 3) exhibit a tensile strength at 300 °C, which is higher than that of sample 8 at room temperature.

SEM observations indicated that the tensile fracture surfaces of various composites were quite different. Many brittle fractured blocks with a size of about 20 μm were found on the fracture surface of sample 8, and secondary cracks were also found on the fractured blocks (Fig. 6a). The energy-dispersive X-ray analysis (EDAX) proved them to be Al_3Ti. It is obvious that the brittle Al_3Ti blocks are the weakest zones in the composites, their earlier brittle fracture results in the fracture of the composites. A few fine Al_2O_3 particulates can be seen on the fractured Al_3Ti blocks and in the fine dimples. After the content of Al_3Ti was reduced to 7.91 vol %, the large fractured Al_3Ti blocks were mostly eliminated (Fig. 6b). The tensile fracture surface of the composite (sample 4) mainly consisted of fine dimples. Only a small amount of the smaller fractured Al_3Ti blocks can be found, indicating that the harmful effect of the blocky Al_3Ti on the properties of the composite was mainly eliminated. The morphologies of the fracture surface of the composite varied little with decreasing Al_3Ti content (Fig. 6c). When the molecular ratio of the B/TiO_2 reached 2/1, no fractured Al_3Ti blocks were found on the tensile fracture surface of the composite (sample 3), the fracture surface consisted of the fine dimples and a few

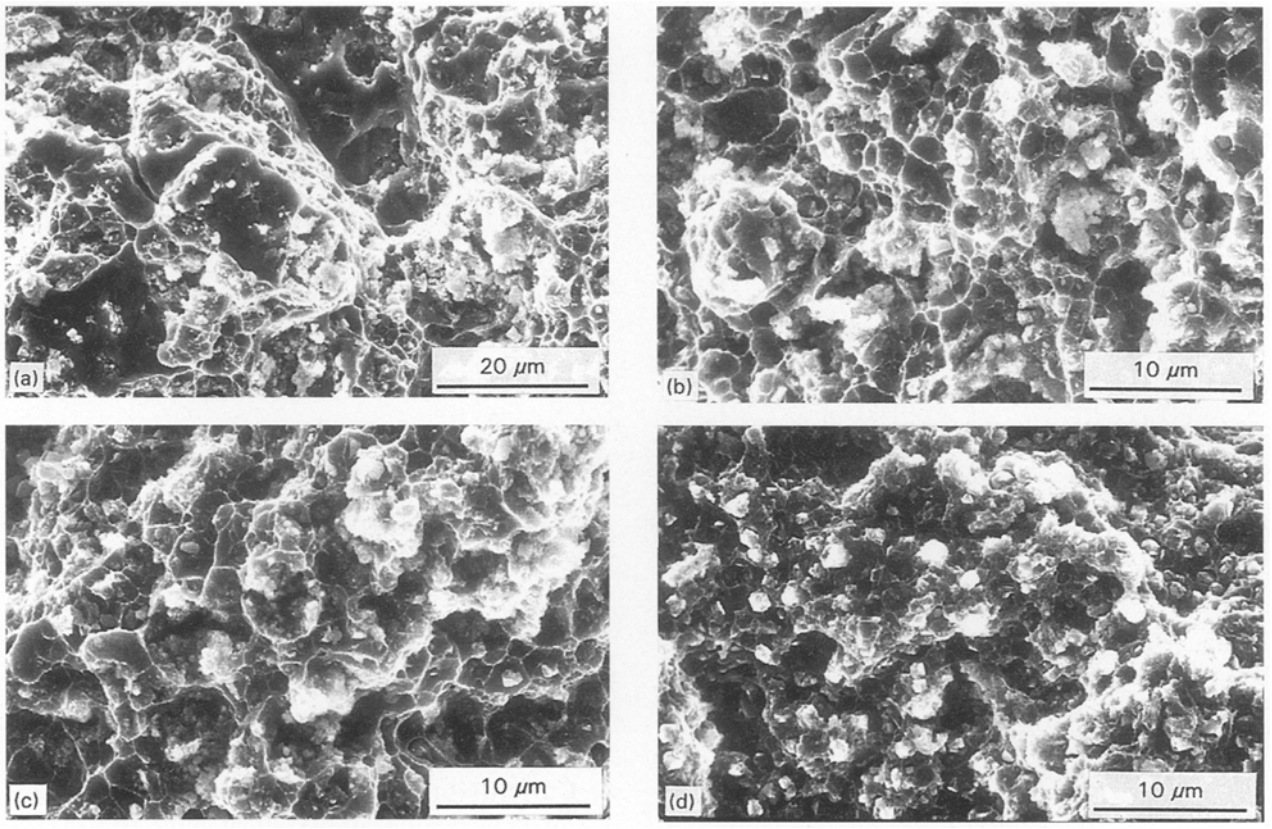

Figure 6 SEM images of tensile fracture surfaces: (a) sample 8, (b) sample 4, (c) sample 5, (d) sample 3.

particulates were pulled out (Fig. 6d). The fine dimple morphologies suggested a good interfacial bonding between particulate and matrix and indicated that the composite would have a high strength.

According to the literature [9], the yield strength in particulate composites is basically related to the particulate–dislocation interaction by means of the Orowan bowing mechanism [10]

$$\tau = \tau_s + \frac{T}{\boldsymbol{b}L/2} \tag{1}$$

where τ is shear yield stress, τ_s the threshold shear stress associated with Orowan bowing, $\boldsymbol{b}$ the Burgers vector, T the line tension of a dislocation, and L the mean interparticle distance. L can be calculated from

$$L = \left(\frac{6}{\pi}V\right)^{-1/3} d_m \tag{2}$$

where V is the volume fraction of the particulates and d_m is the mean particulate diameter. Then, the shear yield strength is given by

$$\tau = \tau_s + \frac{2T}{\boldsymbol{b}d_m}\left(\frac{6}{\pi}V\right)^{1/3} \tag{3}$$

It is assumed that the increase in the yield strength of the composites is mainly due to the increase in TiB_2 content and the Orowan mechanism plays a key role in the process. The shear yield strength of the composites in Equation 3 can be rewritten as

$$\tau = \tau_s + KV_t^{1/3} \tag{4}$$

where K stands for $(2T/\boldsymbol{b}d_m)(6/\pi)^{1/3}$. V_t is the TiB_2 volume fraction. Because the diameter of the TiB_2 particulates does not change much, as observed, in a first approximation, the coefficient K could be considered as a constant.

According to Equation 4 the yield strength of the composites, σ_y, can be written as

$$\sigma_y = \sigma_s + CV_t^{1/3} \tag{5}$$

where σ_s is the yield strength of the composite without TiB_2 and C is a constant. The best fit coefficients in Equation 5 could be found as

$$\sigma_y = 110 + 97.15V_t^{1/3} \tag{6}$$

Fig. 7 shows the effect of TiB_2 content on the yield strength of the composite. It is found that the calculated values in Equation 6 are in fair agreement with experimental results. For the present composites, the ultimate tensile strength is mainly affected by the fracture of large and brittle Al_3Ti particles.

Quantitative metallographic studies on broken specimens as well as *in situ* observations indicated that the fracture stress of brittle particles embedded in a matrix follows the postulates of the Weibull statistics [11, 12]. The probability of fracture, F, for Al_3Ti particles of volume V subjected to an average tensile stress $\bar{\sigma}_p$ is given by [13]

$$F = 1 - \exp\left[\frac{-V}{V_0}\left(\frac{\bar{\sigma}_p}{\sigma_0}\right)^m\right] \tag{7}$$

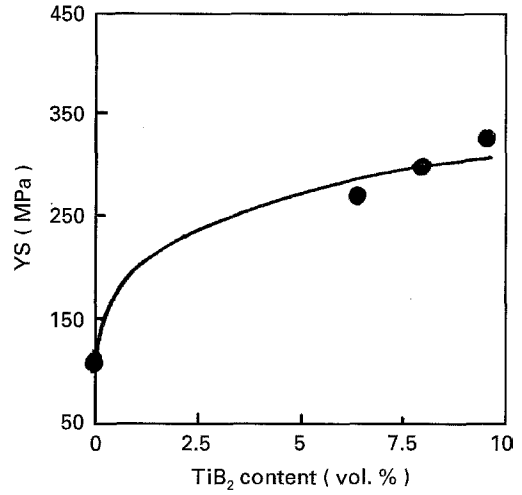

Figure 7 Effect of TiB_2 content on the yield strength of the composites.

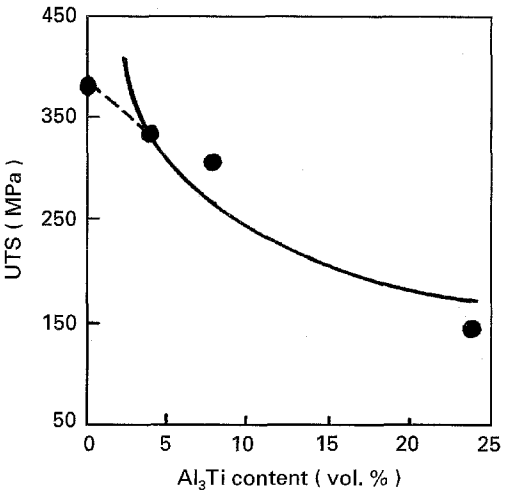

Figure 8 Effect of Al_3Ti content on the tensile strength of the composites.

where m is the Weibull modulus, V_0 and σ_0 are two constants with dimensions of volume and stress, respectively. It is assumed that all the composites fracture under a certain probability of fracture of Al_3Ti particles, then

$$\exp\left[\frac{-V}{V_0}\left(\frac{\bar{\sigma}_p}{\sigma_0}\right)^m\right] = c \tag{8a}$$

or

$$\bar{\sigma}_p = CV^{-1/m} \tag{8b}$$

where c and C are constants.

Because the fracture of Al_3Ti particles leads to the fracture of the composites, the ultimate tensile strength of the composites, σ_c, is proportional to the average tensile stress, $\bar{\sigma}_p$, acting on the Al_3Ti particles, hence

$$\sigma_c = KV^{-1/m} \tag{9}$$

The m values are usually between 1 and 6 [12]; here, an average $m = 3$ is used. The best fit coefficient in Equation 9 could be found as

$$\sigma_c = 518.4V^{-1/3} \tag{10}$$

Fig. 8 shows the effect of the Al_3Ti content on ultimate tensile strength of the composites. The calculated values in Equation 10 are basically in fair agreement with the experimental ones. However, when the content of Al_3Ti particles is very low ($V \to 0$), the equation is not applicable, because the high stress results in the fracture of the composite matrix preferentially, as shown in Fig. 8 by the dotted line.

Although the present models do not give a precise prediction of the relationship between the strength and volume fraction of particles, the general trends, i.e. the yield strength increase with increasing TiB_2 contents, the ultimate tensile strength decrease with Al_3Ti content increase, are well modelled by Orowan dislocation bowing and fracture of brittle particles mechanisms, respectively.

Because the yield and fracture behaviours are very complicated in this kind composite, further work is still required.

4. Conclusions

1. With increasing boron content in the TiO_2–B–Al system, the amount of *in situ* formed TiB_2 particulates increases and the large Al_3Ti blocks are refined and disappear gradually; the distribution uniformity of the *in situ* formed Al_2O_3 and TiB_2 particulates is obviously improved.

2. When the molecular ratio of the B/TiO_2 in the TiO_2–B–Al system reaches 2/1, the Al_3Ti in the composite can be completely eliminated, and the Al_2O_3 and TiB_2 particulates with an average size of 0.31 μm are uniformly distributed in the aluminium matrix.

3. The interface between the *in situ* formed particulate and aluminium matrix is clean. No consistent crystallographic orientation relationship is found.

4. A large amount of Al_3Ti in the composite has no obvious beneficial effect on the strength and modulus of the composite. The strength and modulus can be significantly improved by incorporating boron into the TiO_2–Al system, and the ductility varies slightly.

5. The composites exhibit the excellent elevated temperature strength up to 300 °C after incorporating boron into the TiO_2–Al system.

6. With increasing TiB_2 content in the composites, the morphologies of the tensile fracture surfaces of the composites change from large fractured Al_3Ti blocks and fine dimples to fine dimples and pulled out particulates.

7. With increasing TiB_2 content in the composites, the yield strength of the composite increases, and the tensile strength decreases as Al_3Ti content increases, which is modelled by Orowan dislocation bowing and fracture of brittle particles mechanisms, respectively.

Acknowledgement

This work was supported by a grant from the Director of Foundation Institute of Metal Research, Chinese Academy of Sciences, to whom we are very grateful.

References

1. A.R.C. WESTWOOD, *Metall. Trans.* **19A** (1988) 749.
2. A.K. KURUVILLA, K.S. PRASAD, V.V. BHANUPRASAD and Y.R. MAHAJAN, *Scripta Metall. Mater.* **24** (1990) 873.
3. H. FUKUNAGA, X. WANG and Y. ARAMAKI, *J. Mater. Sci. Lett.* **9** (1990) 23.
4. P.C. MAITY, S.C. PANIGRAHI and P.N. CHAKRABORTY, *Scripta Metall. Mater.* **28** (1993) 549.
5. Z.Y. MA, J.H. LI, M. LUO, X.G. NING, Y.X. LU, J. BI and Y.Z. ZHANG, *ibid.* **31** (1994) 635.
6. Z.Y. MA, J. BI, Y.X. LU, H.W. SHENG and Y.X. GAO, *Acta Metall. Sinica* **6B** (1993) 122.
7. P. SAHOO and M.J. KOCZAK, *Mater. Sci. Eng.* **A131** (1991) 69.
8. G.M. VELETEL, J.E. ALLISON and D.C.V. AKEN, *Metall. Trans.* **24A** (1993) 2545.
9. R.J. ARSENAULT, *Mater. Sci. Eng.* **64** (1984) 171.
10. E. OROWAN, in "Symposium on Internal Stress in Metals and Alloys" (Institute of Metals, 1948) p. 451.
11. D. J. LLOYD, *Acta Metall. Mater.* **39** (1991) 59.
12. T. MOCHIDA, M. TAYA and D.J. LLOYD, *Mater. Trans. JIM.* **32** (1992) 931.
13. J. LLORCA, *Acta Metall. Mater.* **43** (1995) 181.
14. K. WALLIN, T. SAARIO and K. TÖRRÖNEN, *Int. J. Fract.* **32** (1987) 201.

Received 27 June 1994
and accepted 22 June 1995